Agronomy Research **14**(S1), 1200–1211, 2016

Optimization of a solar power station with $LiFePO_4$ accumulators

V. Papez[1] and S. Papezova[2,*]

[1]Czech Technical University in Prague, Faculty of Electrical Engineering, Department of Electrotechnology, Technicka 2, CZ 166 27 Pague 6, Czech Republic
[2]Czech University of Life Sciences in Prague, Faculty of Engineering, Department of Electrical Engineering and Automation, Kamycka 129, CZ 165 21, Prague 6 - Suchdol, Czech Republic; [*]Correspondence: papezovas@tf.czu.cz

Abstract. The paper describes the design and construction of an isolated solar power station supplying energy at weekends to a remote location. The system comprises two parts: a photovoltaic system generating electric energy in sunlight, and an accumulator accumulating energy to be permanently available and to be able to supply a peak power of several kW. The design of the system optimized with respect to maximum reliability, ease of operation and minimum purchase costs. The control circuits were therefore constructed by means of simple analog circuits. To use microcomputers, which are nowadays used in battery management systems most often available on the market, is not appropriate. Such a system, compared with a simpler analog system, is less reliable. Power circuits are again designed in order to ensure minimum complexity of the system. The resulting design is absolutely different from conventional designs offered by suppliers of photovoltaic systems. The photovoltaic part of the system is designed for optimum adaptation of the load characteristic of the photovoltaic generator to the charging characteristic of the accumulator. By selecting photovoltaic panels with appropriate parameters and their appropriate interconnection, possibly by an automatic change of their interconnection during the charging cycle, it is possible to achieve more effective utilization of the charging power of the photovoltaic generator than by using charging DC/DC converters. The accumulator used in the system is formed by an assembly of $LiFePO_4$ accumulators which thanks to their outstanding durability in spite of their high price currently show the lowest cost per accumulated kWh.

Key words: $LiFePO_4$ accumulator, solar power, photovoltaic panel characteristic.

INTRODUCTION

The system charging the accumulators with the power from a photovoltaic (solar) generator is usually designed according to the block circuit diagram shown in Fig. 1.

The solar generator is connected to the charged accumulator via a controlled switch-mode DC/DC converter controlled by a microcomputer.

The operating voltages of the solar generator and accumulator, if they are in an area where the DC/DC converter can work, do not play a significant role in the operation of the system. The controlling computer adjusts the operation of the DC/DC converter to optimize it according to the selected criteria.

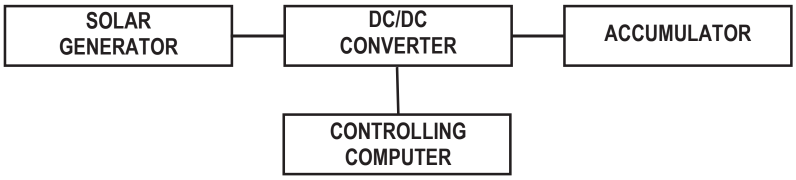

Figure 1. Accumulator charger with a DC/DC converter.

Systems with photovoltaic generators are usually operated in maximum power point tracking (MPPT). The converter transforms the MPP voltage and current from a solar generator to values corresponding to the charging characteristic of the accumulator. Power transmission efficiency reaches up to 98%, as declared by the manufacturers and mainly by the distributors of DC/DC converters for solar systems. In practice, under good conditions, a 90% efficiency (Riawan & Nayar, 2007; Darla, 2007) is reported.

In addition to losses, the main setbacks of these charging systems are the not very high reliability of comprehensive computer-controlled systems and high acquisition costs. Approximately the same efficiency can be achieved without using a DC /DC converter and without the mentioned setbacks if the load characteristic of the solar generator and the charging characteristic of the accumulator are chosen to be as close as possible.

MATERIALS AND METHODS

A typical current-voltage characteristic (I–V curve) of a solar panel for a defined lighting and temperature (1,000 Wm^{-2}, 25 °C = STC–standard test conditions), is in Fig. 2. The dependence was determined as an average of measurements on 10 SH-100S5 (Huashun Solar, 2015) panels. The measurements were performed on a PASAN – Sun Simulator IIIc equipment at the Czech Technical University in Prague (CTU in Prague, 2016). A panel comprising photovoltaic in-series connected cells can be represented by an electric model which is similar to the model standardly used for an individual photovoltaic cell shown in Fig. 3.

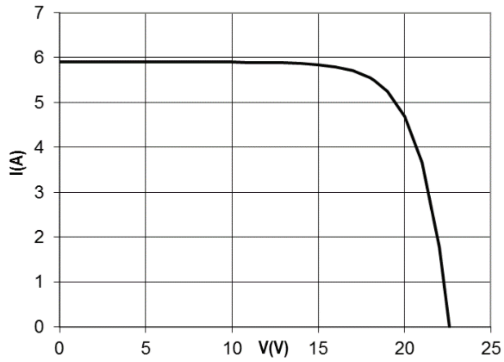

Figure 2. Example of a solar panel load characteristic.

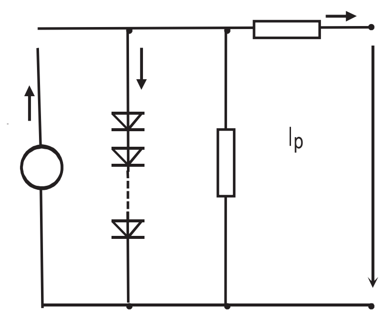

Figure 3. Electric model of a solar panel.

The current from photoelectric cells represents the source of current, a diode string N represents forward biased cell PN junctions, resistance R_s represents the resistance of the interconnecting panel array and resistance R_p represents parallel leak resistances in the panel. The current I supplied by the panel at a terminal voltage V can be expressed by (1). The magnitude of the photovoltaic current I_{ph} is almost proportional to the lighting of the panel. The characteristic of N diodes is expressed in the form of a Shockley approximation of the I–V PN junction characteristic corrected by the ideality factor n of the diode junction, $1 \leq n \leq 2$. Its temperature dependence is represented by the temperature dependence of the terminal voltage of the panel. In practical use the influence of parallel resistance is neglected and thus the last term in equation (1) is eliminated. Also the terminal voltage can be expressed from the simplified equation as a function of the current (2).

$$I = I_{ph} - I_o \left[\exp\left(\frac{e(V + IR_s)}{NnkT} \right) - 1 \right] - \frac{V + IR_s}{R_p} \tag{1}$$

where: I – output current of the solar array (A); I_{ph} – current of the solar array proportional to light intensity (A); I_o – diode saturation current; R_s and R_p – equivalent series and parallel resistance (Ω); N – number of series cells in the solar array; n – diode ideality factor; k – Boltzman constant ($k = 1.381 \text{ x } 10^{-23}$ J K^{-1}); e – electronic charge ($e = 1.602 \text{ x } 10^{-19}$ C); T – cell temperature (K); V – output voltage of the solar array (V).

$$V = \frac{NnkT}{e} \ln\left(\frac{I_{ph} + I_o - I}{I_o} \right) - IR_s \quad \text{if } R_p \to \infty \tag{2}$$

The electrical output P supplied by the panel can be expressed in the form of (3). A typical diagram of the dependence of the proportional output power supplied by the panel on the load current is shown in Fig. 4. The maximum power point tracking current I_{MPP} is almost directly proportional to the lighting of the panel and only to a very low extent depends on the working temperature of the panel.

$$P = VI = \left[\frac{NnkT}{e} \ln\left(\frac{I_{ph} + I_o - I}{I_o} \right) - IR_s \right] I \tag{3}$$

The state when the panel gives maximum output (P_{MPP}) can be determined by finding the extreme of function (3) according to equation (4).

$$\frac{\partial P}{\partial I} = \left[\frac{NnkT}{e} \ln\left(\frac{I_{ph} + I_o - I}{I_o} \right) - IR_s \right] - I \left[R_s + \frac{NnkT}{e(I_{ph} + I_o - I)} \right] = 0 \tag{4}$$

The dependence of the proportional output power of the panel on the load voltage is similar and is illustrated in Fig. 4.

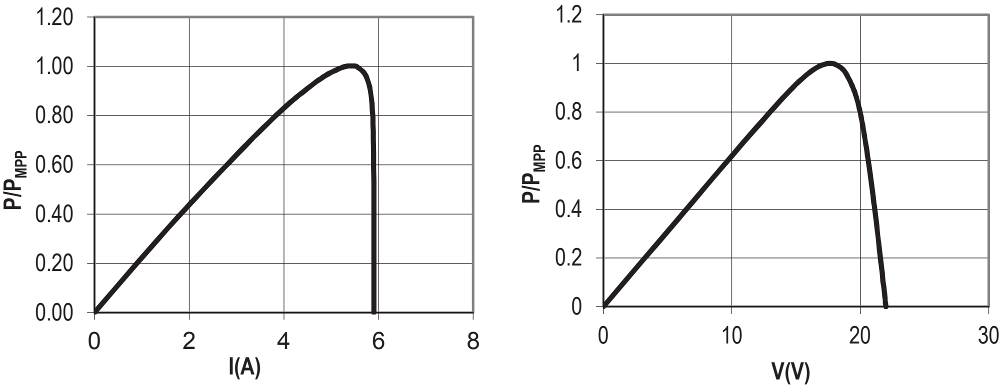

Figure 4. Dependence of the proportional output power on the current and load voltage for panel SH-100S5 (Huashun Solar, 2015) with an *I-V* curve according to Fig. 2.

The voltage V_{MPP} depends on the panel lighting only to a very low extent; at a constant temperature, it is also almost constant. The temperature dependence of V_{MPP} corresponds to the temperature dependence of the voltage on the forward biased p-n junction. In the temperature range where the panel can operate; i.e. from 0 °C to 75 °C, the value of V_{MPP} decreases by about 30% of P_{MPP}, similarly as the maximum output V_{MPP}.

At a constant temperature a PV panel gives an output greater than 90% of P_{MPP} in voltage ranges around V_{MPP}, the width of which is approximately 25% of V_{MPP}. Considering the above mentioned facts, in order to achieve maximum power transfer from the panel to the energy consumer, it is more advantageous to load the panel with a load where the constant terminal voltage is independent of the passing current.

CHARGING ACCUMULATORS FROM THE SOLAR GENERATOR

A typical dependence of the voltage on the supplied charge during the charging of a $LiFePO_4$ accumulator is in Fig. 5.

Voltage depends almost entirely on the supplied charge. The cells show very low internal resistance. In the area of low charging currents, i.e. in case the charging current changes which numerically corresponds to a tenth of the ampere-hour cell capacity, the terminal voltage changes by less than 1%. In the case of constant current charging the voltage of a cell during 96% of the charging time is in a band 25% wide around the mean value. During 90% of the charging time the voltage is in a band 10% wide around the mean value.

If the solar generator and the accumulator are assembled in a way that V_{MPP} is approximately the same as the charging voltage of the accumulator in the middle of the charging cycle, the solar generator will supply up to 96% of P_{MPP} during the charging time. In this case, the efficiency of power transfer from the solar generator to the accumulator can be higher than with the DC/DC converter.

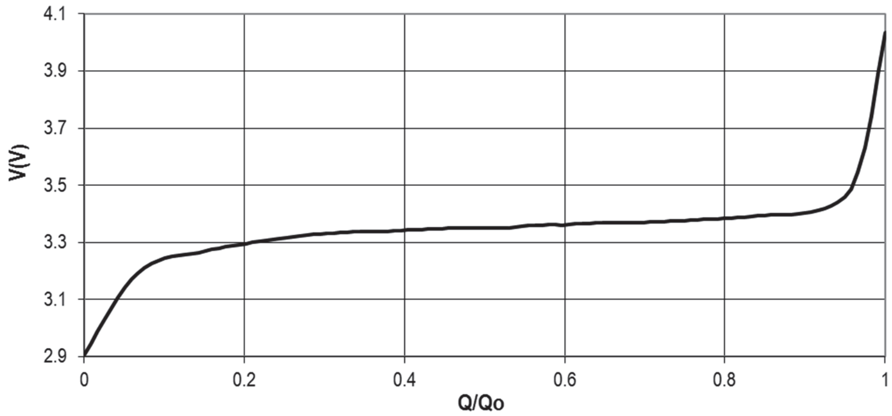

Figure 5. Typical dependence of voltage on the supplied charge during charging (Thunder Sky, 2015; Global World Logistic, 2015).

Nevertheless, the situation is complicated by the temperature dependence of the solar generator. Both V_{MPP} and output depend on the instantaneous temperature of the photovoltaic cells, whereas the temperature further depends on the ambient temperature, sunshine intensity and technique of the solar generator assembly and speed of the wind. The typical dependence of P_{MPP} on the terminal voltage for different temperatures of solar panel cells is in Fig. 6.

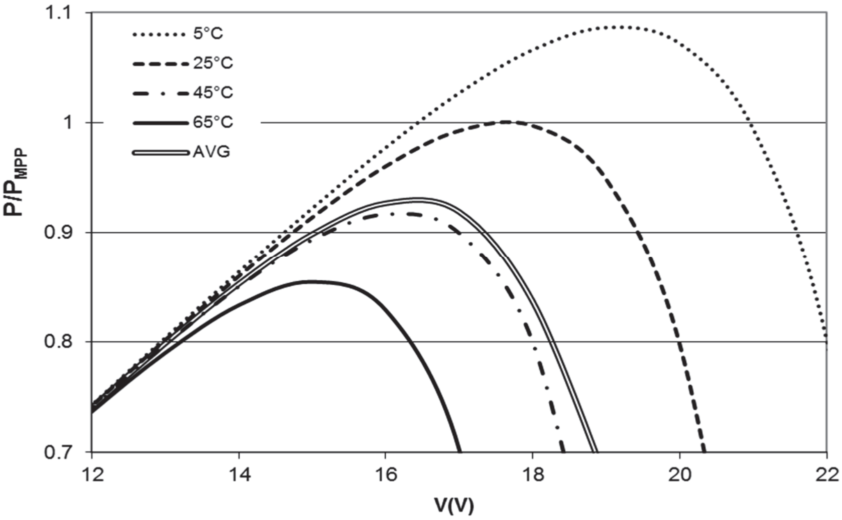

Figure 6. Typical dependence of P_{MPP} on the terminal voltage for different temperatures of the solar panel cells SH-100S5 (Huashun Solar, 2015).

The stated temperatures represent typical temperatures of solar cells in various seasons with regard to the temperature and sunlight. A 5 °C temperature represents winter, 25 °C and 45 °C temperatures represent transitional periods both in autumn and spring, and a 65 °C temperature represents summer. The annual average was weighted with respect to the operating time of panels at temperatures considered during the year. It is obvious that due to the temperature dependence of V_{MPP}, a high level of efficiency of the solar panels can be achieved only in a narrower range of temperatures. At higher temperatures, exceeding approximately 50 °C, the lower output voltage of the solar generator would not be sufficient to charge the accumulator fully.

The solution might be to design a solar generator in a way that its load characteristic (*I–V* curve) in a wide temperature range would be similar to the charging characteristic of the accumulator. Charging the accumulator fully can be reached by adjusting the voltage levels. The efficiency of the charging process can be optimized by adjusting the current temperature dependences.

The issue of the optimal adaptation of the solar generator characteristic and that of the accumulator was solved by assembling the generator from conventional 36–cell panels and their series–parallel interconnection into two different branches interconnected via a diode gate. Such an optimization can also be achieved by the choice of the number of $LiFePO_4$ cells.

Optimization of the solar generator design was performed by simulations according to the measured characteristics both of the solar panels and accumulators for different operating temperatures of the panels and for different nominal currents on the branches of the solar generator.

If the average voltage during the charging and the maximum charging voltage are considered, the ratio of the operating voltages of both branches close to the value of 1.2 can be determined by evaluating the voltages during the charging of the $LiFePO_4$ accumulator. When conventional panels were used we selected a variant with the first branch with 4 in-series connected panels (i.e. panel groups), and the second branch with 5 in-series connected panels. The number of accumulator cells and the ratio of the nominal currents of the branches were chosen as simulation parameters. With respect to standard climatic conditions in the time of operation of the system, the operating cell temperature was set in the range 5 °C – 65 °C. In order to analyze the simulation, the ratio was chosen between the power transferred to the accumulator during charging and the maximum energy which could be supplied by the solar generator. The energy was taken as a product of the charging period and P_{MPP}. This product is hereafter denoted as the system efficiency.

The results of the simulation for a 20–cell accumulator, at temperatures within the selected range and the nominal current of the branch with higher voltage in the range from 0 to a value equal to the nominal current of the second branch, are summarized in the diagram in Fig. 7. It is obvious that at operating cell temperatures in the range 25 °C – 45 °C, an efficiency exceeding 95% can be achieved provided the relation of the nominal voltages of the generator and accumulator are chosen appropriately.

At a low temperature the operating conditions of the system do not change significantly. The system efficiency decreases by about 5% as V_{MPP} increases with a decrease of the temperature and the voltage on the accumulator terminals is temperature-independent.

A different situation occurs at high operating cell temperatures. The decrease in V_{MPP} and open-circuit voltage leads to a situation when the charging current of the first branch of the solar generator rapidly decreases or even approaches zero at the end of charging. The charging is then completed only by the current from the second branch. Higher efficiency in this area is achieved by selecting a higher nominal current of the second branch. Hence the charging process is shortened and likewise the time, when the first branch operates no-load (YEAR).

The graph in Fig. 7 shows the average values of efficiency corresponding to the weighted averages of all considered temperature dependences. The behaviour marked by YEAR represents the average values at a higher share of the transitional periods, i.e. temperatures 25 °C and 45 °C and SUMMER represents the average values at a higher share of summer, i.e. temperature in the range 45 °C – 65 °C.

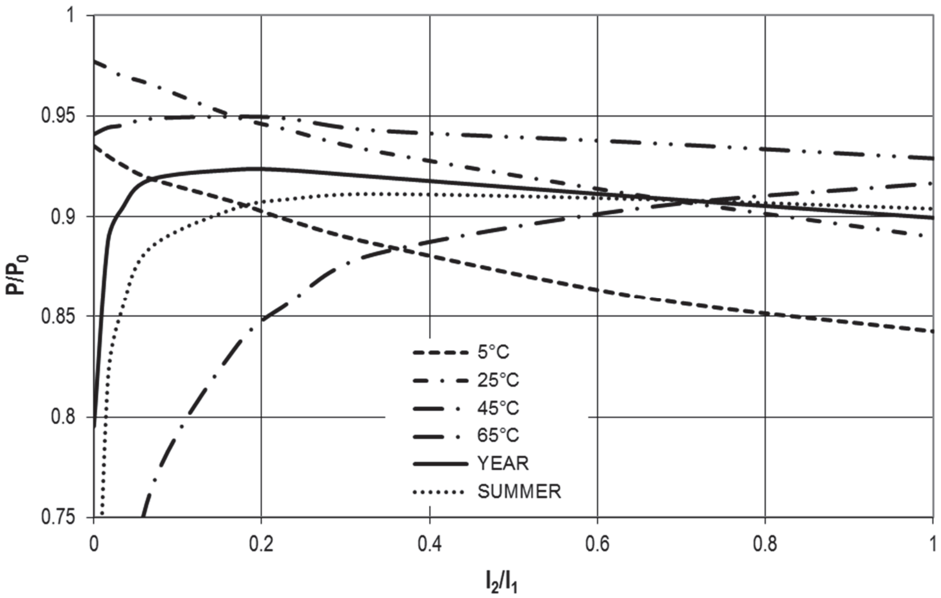

Figure 7. Dependence of the efficiency of the solar system on the ratio of the currents of the branches for different cell temperatures.

The final evaluation of the two curves is approximately the same: nominal current of the second branch should be selected as 1/3 or 1/2 of the nominal current of the first branch. An achievable average value of the efficiency of the system for the whole year ranges from 90% to 92%. As stated earlier, the solar power system can reach approximately the same efficiency without using a DC/DC converter to match the solar generator and accumulator. The advantage of the system with the matched generator and accumulator is its lower purchase cost and significantly higher reliability compared with the system using the DC/DC converter. Moreover, any interference caused by the DC/DC converter switches and all problems associated with the suppression of interferences are eliminated.

System controlling circuits

An analog control system based on the design described in (Papež & Papežová, 2015) is used to control the operation of the accumulator. Microcomputer systems which are now currently available on the market (Petchjatuporn et al., 2005) cannot be recommended for an unattended control system since they are much less reliable than simpler analogue systems. The reliability of their operation is also reduced by the influence of external atmospheric and random disturbances. If other electronic devices processing low level signals work in their vicinity, the radiation of the timing signal from the microcontroller and its harmonic signals can cause such interference.

The evaluation of the required actual limiting values is performed by simple analog comparators the output signal of which is processed by conventional combinatory circuits. All protective circuits starting from the comparators up to the power switches are duplicated and sometimes triplicated in order to ensure maximum reliability of the control of the operation of the accumulator. A block diagram of the control system is in Fig. 8.

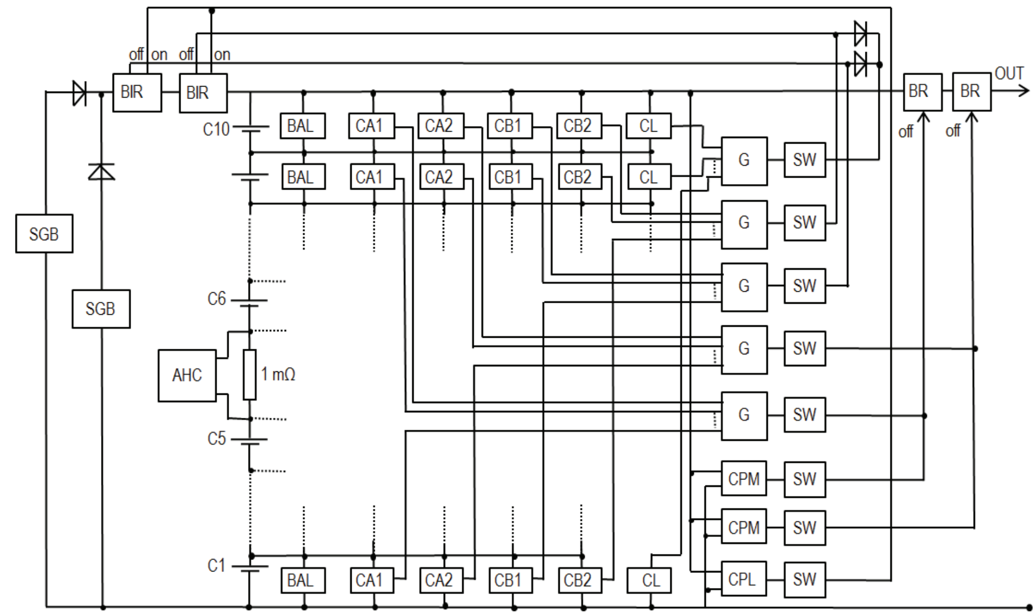

Figure 8. Block diagram of the control system: AHC – ampere-hour counter; BAL – balancer; BIR – bistable relays; BR – breaker; C1 – C10 accumulator cells; CA1, CA2 – minimum cell voltage sensors; CB1, CB2 – maximum cell voltage sensors; CL – charging–off cell voltage sensors; CPL – charging –on accumulator voltage sensor; CPM – accumulator voltage minimum sensor; G – analog gate; SGB – solar generator branch; SW – relay coil current switch.

The control system comprises five comparator networks independently evaluating voltages of individual cells the signals of which are combined and evaluated together and three independent comparators evaluating the total voltage of the accumulator.

Tested values

The minimum voltage of individual cells of the accumulator is evaluated by two independent comparator networks which at a risky drop of the voltage on one of the cells turns off two series-connected circuit breakers.

The minimum voltage of the accumulator is simultaneously evaluated by two independent comparators which independently turn off the same series-connected circuit breakers just as the previous network has done it.

The maximum voltage of individual cells of the accumulator is evaluated by two independent comparator networks which, when one of the cells is overcharged, turns off two series-connected bistable relays and thus disconnects the charging.

The final charging voltage of individual cells is evaluated by a comparator network. When all accumulator cells are fully charged the identical series-connected bistable relays are independently turned off in the same way as in the previous network.

The starting voltage for charging the accumulator is evaluated by a comparator which turns on the bistable relays connecting the solar generator during charging.

The issue of preventing cells which are not entirely identical from overcharging is solved by their balancing. Balancing is provided by passive balancers (Papež & Papežová, 2015; Albertronic, 2015). When the voltage of the cells reaches a value signifying that they are charged, the balancers draw the charging current supplied by the PV panels from the cells of the accumulator. Charging continues until the voltage of all cells reaches the value corresponding to the charge and all cells are fully charged.

Measurements show that the average time the balancer operates on all cells in the accumulator is approximately 1% of the charging time of the accumulator. The total energy consumed by the balancers from all accumulator cells is about 1.2% of the energy necessary for charging the accumulator. This is because the balancers operate at the end of the charging cycle when the cells are loaded with the highest voltage.

The state of the accumulator during the operation is evaluated by an Up/Down ampere-hour counter which indicates the charge available in the accumulator.

RESULTS AND DISCUSSION

A solar power station was built as a source of electricity at weekends for an amateur radio station and other facilities in a remote location. For economical reasons the system was designed as a half of the optimal configuration described above.

The accumulator comprises 10 WB- LYP300AHA Winston Battery cells (300 Ah capacity, average discharge voltage about 3.15 V, (Global World Logistic, 2015; Thunder Sky, 2015)), see Fig. 9.

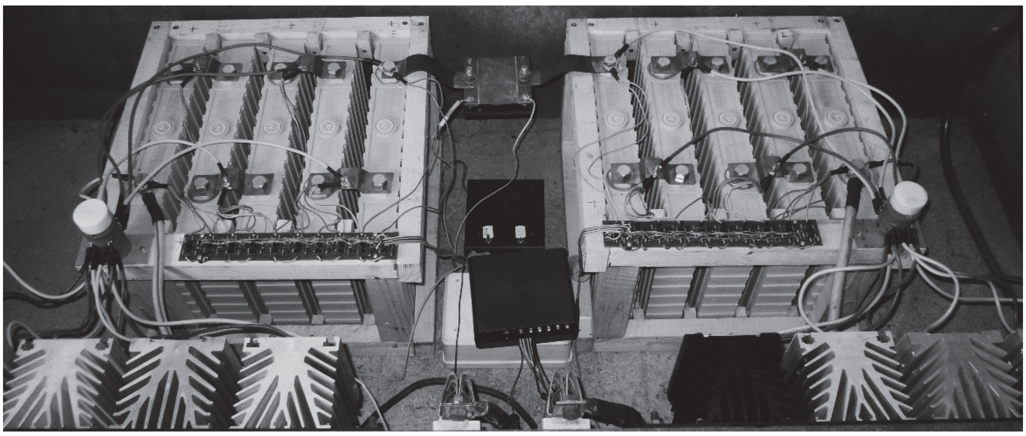

Figure 9. Accumulator of the solar power station.

The solar generator consists of 9 type SH-100S5 Ningbo Huashun Solar Energy Technology Co., Ltd. solar panels (see Fig. 10). The panel is equipped with 36 cells (125 x 125 mm). Under standard conditions, it supplies 100 W at a 18.25 V voltage (Huashun Solar, 2015). The panels are interconnected in two branches: 1) a low voltage branch with 3 in-parallel connected groups each comprising 2 in-series connected panels and 2) a high-voltage branch comprising 3 panels connected in series. The high voltage branch has an operating voltage corresponding to a 1.5 multiple of the voltage on the low voltage branch, i.e., higher than the optimum voltage, which results in a reduction of the efficiency of the system by about 5% compared with the theoretical value.

Figure 10. Solar generator of the solar power station.

The state of the charge of the accumulator in a solar power station for standard operation of the amateur radio station at weekends from May to December 2015 is in Fig. 11.

Sharp charge drops indicate the accumulator discharge during a radio amateur contest when the transmitter consumes a peak power of up to 3 kW. After that the accumulator is fully charged by the solar system. In summer the longest charging time is 5 days with an 85% discharge. In autumn (November) charging lasts about 12 days with a 50% discharge.

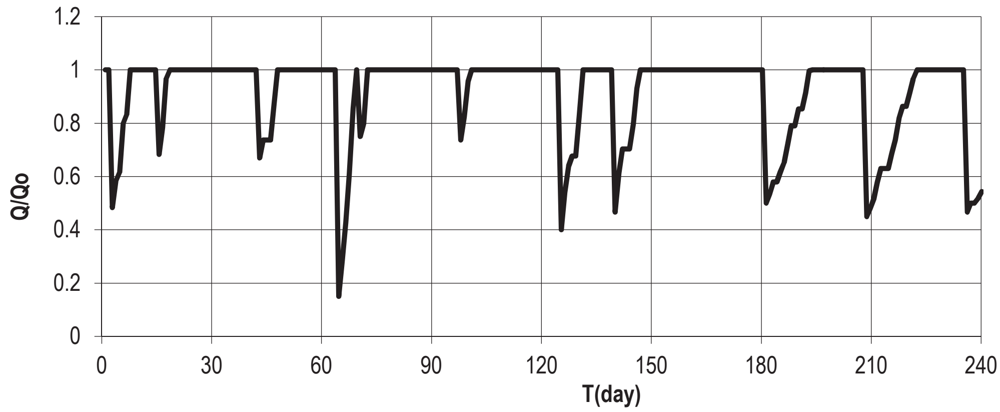

Figure 11. Accumulator charge level in May-December, 2015.

CONCLUSIONS

The design of the PV power station described in the present paper consistently avoids the use of controlling switch-mode DC/DC controllers and controlling microcomputers. The described analog system utilizes exclusively linear control. When the parameters of the PV generator and accumulator are appropriately selected this system has approximately the same efficiency as the system with pulse control for which maximum efficiency is usually assumed.

An advantage of the design of the analog system, compared with the pulse system, is the negligible risk of production of disturbing signals and higher reliability of the simpler analog system.

A complete review of the properties of the designed system will be possible only after the evaluation of the life of the accumulator which is the most expensive component of the system.

ACKNOWLEDGEMENTS. Thanks for cooperation are due to the Laboratory of Photovoltaic Systems Diagnostics, Faculty of Electrical Engineering, Czech Technical University in Prague and Faculty of Engineering, Czech University of Life Sciences in Prague, IGA 31200/1312/3118.

REFERENCES

Albertronic, B.V. http://www.123electric.nl. Accessed 22.12.2015.

CTU in Prague, Faculty of Electrical Engineering, Laboratory of Photovoltaic Systems Diagnostics http://pasan.feld.cvut.cz/en/index.html. Accessed 22.03.2016.

Darla, R.B. 2007. *Development of Maximum Power Point Tracker for PV Panels Using SEPIC Converter*. In: 29th International Telecommunications Energy Conference. INTELEC 2007. IEEE. Roma. pp. 650–655.

Global World Logistic Ltd. http://www.ev-power.eu/docs/GWL-LFP-Product-Spec-260AH-7000AH.pdf. Accessed 22.12.2015.

Ningbo Huashun Solar Energy Technology Co., Ltd. http://www.enfsolar.com/pv/panel-datasheet/Monocrystalline/10875. Accessed 22.12.2015.

Papez, V. & Papezova, S. 2015. Isolated Solar Power Station. In: *14th International Scientific Conference Engineering for Rural Development Proceedings*. Latvia University of Agriculture. Jelgava. pp. 458–465.

Petchjatuporn, P., Sirisuk, P., Ngamkham, W., Kiranon, W., Khaehintung, N. & Kunakorn, A. 2005. *A Solar-powered Battery Charger with Neural Network Maximum Power Point Tracking Implemented on a Low-Cost PIC-microcontroller* In: International Conference on Power Electronics and Drives Systems. PEDS2005. IEEE. Kuala Lumpur, pp. 507–510.

Riawan, D.C. & Nayar, C.V. 2007. *Analysis and Design of a Solar Charge Controller Using Cuk Converter*. Power Engineering Conference. AUPEC 2007. Australasian Universities. IEEE. Perth, pp. 1–6.

Thunder Sky Winston Battery. http://en.thunder-sky.com/index.php/products/download-center/category/battery-lyp. Accessed 22.12.2015.